Research Square

Preprints are preliminary reports that have not undergone peer review.
They should not be considered conclusive, used to inform clinical practice,
or referenced by the media as validated information.

Connectome Harmonic Analysis at 7 Tesla Reveals Selective Reorganization of Large-Scale Cortical Dynamics in Adult Users of Cannabis.

Alan Francis

alan.francis@utrgv.edu

University of Texas Rio Grande valley https://orcid.org/0000-0001-8851-0758

Francesca Filbey

The University of Texas at Dallas

Ihsan Salloum

https://orcid.org/0000-0001-7318-9316

Article

Keywords:

Posted Date: November 20th, 2026

DOI: https://doi.org/10.21203/rs.3.rs-11021187/v1

License: This work is licensed under a Creative Commons Attribution 4.0 International License.
Read Full License

Additional Declarations: The authors have declared there is **NO** conflict of interest to disclose

Connectome Harmonic Analysis at 7 Tesla Reveals Selective Reorganization of Large-Scale Cortical Dynamics in Adult Users of Cannabis.

Alan N. Francis, PhD[1]; Francesca M. Filbey, PhD[2]; Ihsan M. Salloum, MD, MPH[1]

[1]Institute of Neuroscience, School of Medicine, University of Texas Rio Grande Valley, TX.

[2]Center for Brain Health, School of Behavioral and Brain Sciences, University of Texas at Dallas, TX.

Corresponding Author:

Alan N. Francis, PhD,

Department of Neuroscience,

School of Medicine,

University of Texas Rio Grande Valley,

1201 W University Dr, Edinburg, TX 78539, USA.

Email: alan.francis@utrgv.edu

Abstract

Background

Cannabis exposure is associated with altered functional connectivity, cognitive impairment, and psychosis-spectrum risk, but the systems-level principles through which it reshapes large-scale brain organization remain poorly understood. Connectome Harmonic Analysis (CHA), a spectral graph-theoretic framework, characterizes the intrinsic spatial modes governing cortical communication. We investigated whether cannabis use alters low-frequency connectome harmonics using ultra-high-field 7 Tesla MRI.

Methods

Resting-state fMRI and high angular resolution diffusion data from the Human Connectome Project 7T cohort were used for Connectome Harmonic Analysis in 81 cannabis users (CU) and 81 matched non-users (NU). BOLD activity was projected onto the first 200 connectome harmonics; group differences in harmonic power were assessed with independent-samples t-tests and FDR correction, and significant harmonics were anatomically localized using the HCP multimodal parcellation atlas.

Results

Cannabis users exhibited significantly increased power in a single low-frequency connectome harmonic ($k = 6$; $\lambda_6 = 0.01144$; $t \approx 4.19$; $p_{FDR} = 7.21 \times 10^{-3}$; Cohen's $d = 0.659$), reflecting approximately 44% greater normalized power than non-users; no higher-frequency harmonics survived correction. This harmonic localized to a distributed frontoparietal–sensorimotor network spanning bilateral premotor, supplementary motor, and superior parietal cortex, intraparietal sulcus, and supramarginal gyrus, and did not correlate with cannabis clinical exposure variables (age at onset, duration, frequency, or abuse/dependence diagnosis; all $\rho < 0.09$, $p > 0.44$). Behavioral correlation analyses revealed nominal, domain-specific associations — slower working memory reaction time across the cohort ($\rho = +0.18$, $p = 0.026$), greater ADHD symptom burden ($\rho = +0.23$, $p = 0.041$) and extraversion ($\rho = +0.25$, $p = 0.026$) in cannabis users, and lower theory-of-mind accuracy in non-users ($\rho = -0.23$, $p = 0.042$) — though standard cognitive composites were null and no association survived FDR correction.

Conclusions

Cannabis use is associated with selective amplification of a low-frequency connectome harmonic subserving frontoparietal–sensorimotor integration, suggesting that cannabis exposure alters the brain's intrinsic dynamical architecture at the level of macroscale eigenmodes rather than isolated regional circuits. Connectome harmonics may thus provide a systems-level biomarker linking cannabinoid neurobiology to cortical coordination relevant to psychosis vulnerability, predictive processing abnormalities, and network dysregulation in psychiatric illness.

Keywords

Cannabis; Connectome Harmonics; 7 Tesla MRI; Functional Connectivity; Spectral Graph Theory; Psychosis; Frontoparietal Network; Sensorimotor Integration; Human Connectome Project

Introduction

Cannabis is among the most widely used psychoactive substances globally, with increasing potency and rising rates of regular use raising concerns regarding its long-term neurobiological consequences (Volkow et al., 2014; Hall & Degenhardt, 2009). Epidemiological and longitudinal studies demonstrate associations between frequent cannabis exposure and elevated risk for cognitive impairment, affective dysregulation, psychosis-spectrum symptoms, and altered neurodevelopmental trajectories, particularly when use begins during adolescence (Arseneault et al., 2004; Meier et al., 2012; Murray et al., 2017). Neuroimaging studies have further shown that cannabis exposure is associated with abnormalities in corticolimbic circuitry, salience processing, executive control, reward signaling, and sensorimotor integration (Bloomfield et al.,

2019; Weinstein et al., 2016). However, despite extensive investigation, the systems-level principles through which cannabis reshapes large-scale brain organization remain poorly understood.

Most prior neuroimaging studies of cannabis have relied on regional activation contrasts, seed-based functional connectivity, or graph-theoretic metrics. Although informative, these approaches largely characterize pairwise relationships between discrete regions and may therefore overlook the fundamental spatial modes through which brain activity is coordinated across the cortex. The human brain operates as a hierarchical dynamical system in which neural activity propagates along anatomically constrained gradients and oscillatory modes spanning distributed cortical territories (Margulies et al., 2016; Huntenburg et al., 2018). Understanding how cannabis alters these intrinsic spatial modes may provide a mechanistic bridge between molecular cannabinoid effects and macroscale network dysfunction. Because the brain functions as a dynamic, interdependent system rather than a set of isolated circuits, such a systems-level, harmonic decomposition may offer a more holistic and ecologically representative account of how cannabis reorganizes the neural substrates of behavior than approaches confined to discrete regions or pairwise connections.

Recent advances in spectral graph theory and connectomics have introduced Connectome Harmonic Analysis (CHA) as a powerful framework for characterizing the

brain's intrinsic dynamical architecture (Atasoy et al., 2016; Atasoy et al., 2017). CHA decomposes the structural connectome into eigenmodes of the graph Laplacian—termed connectome harmonics—which represent the fundamental spatial patterns through which neural activity can flow across the cortex. Analogous to harmonic decomposition in acoustics or quantum systems, low-frequency harmonics encode smooth, large-scale cortical gradients, whereas higher-frequency harmonics capture increasingly localized spatial structure. Importantly, resting-state neural activity can be projected onto these harmonics to quantify harmonic power, thereby indexing the degree to which specific intrinsic brain states are preferentially engaged.

This framework has gained increasing relevance in psychiatric and consciousness research because connectome harmonics appear sensitive to alterations in global brain dynamics induced by psychedelics, anesthesia, altered states of consciousness, and neuropsychiatric illness (Atasoy et al., 2017; Luppi et al., 2020; Lord et al., 2019). Harmonic analyses suggest that alterations in the balance between low- and high-frequency spatial modes may reflect changes in cortical integration, hierarchical organization, and excitation–inhibition dynamics. These mechanisms are directly relevant to cannabinoid neurobiology because Δ9-tetrahydrocannabinol (THC), the principal psychoactive component of cannabis, exerts widespread effects on glutamatergic, GABAergic, and dopaminergic signaling through CB1 receptor modulation (Bossong & Niesink, 2010; Bloomfield et al., 2016). CB1 receptors are

densely expressed throughout association cortex, sensorimotor networks, hippocampus, basal ganglia, and thalamocortical circuits, positioning the endocannabinoid system as a major regulator of large-scale cortical coordination (Herkenham et al., 1990; Glass et al., 1997). Cannabis exposure may therefore alter the energetic distribution of intrinsic cortical harmonics, reflecting a systems-level reorganization of brain dynamics. Yet, despite growing interest in connectome harmonics as a systems neuroscience framework, their relationship to cannabis use has not previously been examined.

Ultra-high-field 7 Tesla MRI provides a unique opportunity to investigate these questions with substantially enhanced spatial resolution and signal-to-noise ratio relative to conventional field strengths (Vu et al., 2015; Ugurbil, 2018). Such resolution is particularly advantageous for harmonic analysis because subtle alterations in large-scale cortical gradients and distributed oscillatory modes may otherwise remain obscured. The Human Connectome Project 7T dataset therefore offers an unprecedented platform for examining whether cannabis use is associated with reorganization of the brain's intrinsic harmonic architecture.

In the present study, we applied Connectome Harmonic Analysis to resting-state and HARDI diffusion MRI data acquired at 7 Tesla in a matched cohort of cannabis users and non-users drawn from the Human Connectome Project. We tested whether cannabis use was associated with altered power in specific connectome harmonics and localized the

anatomical substrates of any significant harmonic modes using high-resolution cortical parcellation.

We hypothesized that cannabis users would exhibit significant alterations in low-frequency connectome harmonics reflecting large-scale cortical reorganization rather than focal regional abnormalities. Specifically, we predicted that:

1. Cannabis users would demonstrate increased power within low-order harmonics subserving sensorimotor and frontoparietal integration networks.
2. Harmonic alterations would preferentially involve association cortices implicated in attentional control, salience integration, motor planning, and predictive processing.
3. Cannabis-related harmonic changes would manifest predominantly within spatially smooth, macroscale cortical modes, consistent with altered global coordination of cortical signaling.

The present study was designed to address four principal questions:

1. Does cannabis use alter the intrinsic harmonic architecture of the human connectome?
2. Are cannabis-related effects localized to specific large-scale cortical eigenmodes or distributed diffusely across the harmonic spectrum?

3. Which anatomical systems contribute most strongly to altered harmonic expression in cannabis users?
4. Do connectome harmonics provide a sensitive systems-level biomarker linking cannabis exposure to large-scale cortical dysregulation relevant to psychiatric vulnerability?

METHODS

Participants

Data were obtained from the Human Connectome Project (HCP) 7 Tesla (7T) dataset, an open-access repository of multimodal neuroimaging data acquired in healthy adults (Van Essen et al., 2013). From the full HCP 7T cohort, participants were classified as cannabis users (CU) if they reported at least 10 lifetime uses of cannabis on the SSAGA interview, with use within the preceding 12 months, and as non-users (NU) if they reported no lifetime cannabis use. To ensure group comparability, CU and NU participants were matched 1:1 on biological sex and age using a greedy nearest-neighbour algorithm with replacement prohibited. The final analytic sample comprised 162 participants: 81 CU (mean age 29.7 ± 3.0 years; 49 female) and 81 NU (mean age 29.4 ± 3.5 years; 49 female). Participants with missing structural or functional imaging data, excessive head motion (mean framewise displacement > 0.5 mm), or incomplete HCP preprocessing were excluded prior to matching. All data were collected under protocols approved by the Washington University Institutional Review Board; all participants provided written informed consent.

Data Acquisition

All imaging was performed on a 7T Siemens Magnetom scanner with a 32-channel head coil. Resting-state functional MRI (rs-fMRI) data were acquired using a gradient-echo EPI sequence (TR = 1,000 ms, TE = 22.2 ms, flip angle = 45°, resolution = 1.6 mm isotropic, 85 slices, 900 volumes per run). Two runs of rs-fMRI were acquired per participant in two phase-encoding directions (posterior-to-anterior and anterior-to-posterior). Diffusion-weighted imaging (DWI) was acquired at 1.05 mm isotropic resolution with b-values of 1,000, 2,000, and 3,000 s/mm^2. Full acquisition parameters are described in Vu et al. (2015). All data were preprocessed using the HCP minimal preprocessing pipeline (Glasser et al., 2013), which includes gradient distortion correction, motion correction, registration to MNI152 standard space, surface reconstruction using FreeSurfer, and registration to the fsLR-32k surface template.

Structural Connectome and Connectome Harmonics

Connectome harmonics were computed as the eigenvectors of the normalised graph Laplacian of the individual structural connectome, following the framework of Atasoy et al. (2016, 2017). Briefly, for each participant, whole-brain probabilistic tractography was performed on the preprocessed DWI data to construct a structural connectivity matrix $\hat{} \in \mathbb{R}^n \times ^n$, where each entry encodes the normalised streamline count between pairs of cortical surface vertices on the fsLR-32k mesh (n = 59,412 non-medial-wall vertices across both hemispheres). The normalised Laplacian was defined as $\mathcal{L} = I - D^{-½}\hat{}D^{-½}$, where D is the degree matrix. The K = 200 eigenvectors $\Psi = [\psi_1, \psi_2, \ldots, \psi_{200}]$ with the smallest non-zero eigenvalues $\{\lambda_1 \leq \lambda_2 \leq \ldots \leq \lambda_{200}\}$ were retained as the connectome harmonics. These eigenvectors represent spatially coherent oscillatory modes of the structural connectome, ordered from lowest (most spatially smooth) to highest spatial frequency. Eigenvectors were computed using a sparse eigendecomposition solver (scipy.sparse.linalg.eigsh, Python 3.11).

Harmonic Power Projection

For each participant, the resting-state BOLD timeseries (T × 59,412 matrix, after HCP surface preprocessing and ICA-FIX denoising) was projected onto the K connectome harmonics to obtain a harmonic power spectrum. Specifically, the power associated with harmonic k was defined as:

$$P_k = (1/T) \sum_t (\psi_k^T x_t)^2$$

where $x_t \in \mathbb{R}^n$ is the BOLD signal across all cortical vertices at time t. Power values were normalised across harmonics within each subject to sum to unity, yielding a relative harmonic power spectrum per participant. This normalisation renders the measure invariant to global signal amplitude and enables direct between-subject comparison of harmonic mode engagement.

Group-Level Statistical Analysis

Between-group differences in normalised harmonic power were assessed using independent-samples t-tests (CU vs. NU) at each of the K = 200 harmonics. Multiple comparisons were controlled using the Benjamini–Hochberg false discovery rate (FDR) procedure (Benjamini & Hochberg, 1995) at a threshold of $q < 0.05$. Effect sizes were quantified as Cohen's d. Statistical analyses were implemented in Python 3.11 using SciPy (v1.11) and StatsModels (v0.14).

Spatial Localisation

For each harmonic that survived FDR correction, the corresponding eigenvector was mapped to the fsLR-32k cortical surface to determine the spatial distribution of the associated connectivity mode. To obtain a group-representative spatial map, eigenvectors were sign-aligned across subjects prior to averaging: each individual eigenvector was flipped in sign such that its largest-magnitude component was positive, resolving the arbitrary sign ambiguity inherent to eigendecomposition. Sign-aligned eigenvectors were then averaged across all 162 participants. The resulting group-average eigenvector (59,412 vertices) was saved as a GIFTI metric file (.shape.gii) for

each hemisphere and as a CIFTI dense scalar (.dscalar.nii) for visualisation in Connectome Workbench (Marcus et al., 2011).

Parcellation

To characterize the anatomical distribution of the significant harmonic, the group-average eigenvector was parcellated using the Human Connectome Project Multi-Modal Parcellation version 1.0 (Glasser MMP 1.0; Glasser et al., 2016), which subdivides each hemisphere into 180 cortical areas (360 parcels in total) defined by a combination of cortical architecture, function, connectivity, and topographic organisation. Parcellation label files in fsLR-32k space (.dlabel.nii) were obtained from the BALSA neuroimaging database (https://balsa.wustl.edu, study RVVG). For each parcel, the mean eigenvector weight across all constituent vertices was computed and parcels were ranked by the absolute mean weight to identify regions most strongly engaged by the significant harmonic mode.

RESULTS

Socio-Demographics:

After matching on sex and age, the final sample comprised 81 cannabis users and 81 non-users. Groups were well-matched on demographic characteristics (age: CU mean 29.7 ± 3.0 years vs. NU mean 29.4 ± 3.5 years, $t(160) = 0.53$, $p = 0.60$; sex: 60.5% female in both groups). Cannabis users reported a median age of first use of 18–20 years (SSAGA ordinal category 3; 39.5% initiated before age 18); 13.6% (n = 11) met DSM-IV criteria for cannabis abuse or dependence. No significant between-group differences in head motion (mean framewise displacement: CU = 0.174 ± 0.077 mm, NU = 0.165 ± 0.062 mm) were observed ($t(160) = 0.81$, $p = 0.42$).

Table 1. Demographic Characteristics

Variable	Cannabis Users (n = 81)	Non-Users (n = 81)	Statistic (p)
Age, years (mean ± SD)	29.6 ± 3.8	29.2 ± 3.6	t = 0.31, p = 0.76
Sex, female n (%)	47 (58%)	45 (56%)	χ^2 = 0.00, p = 1.00
Age of first use, median ordinal	2.4 (15–19 yrs)	N/A	—
Lifetime use > 10 times, n (%)	70 (86%)	N/A	—
DSM-IV abuse/dependence, n (%)	11 (13.6%)	0 (0%)	—

Altered Power in Harmonic k = 6

Applying FDR correction across all K = 200 connectome harmonics, one harmonic survived the significance threshold of $q < 0.05$: harmonic k = 6 (eigenvalue $\lambda_6 = 0.01144$; $t \approx 4.19$, df = 160, $p_{FDR} = 7.21 \times 10^{-3}$). Cannabis users exhibited significantly greater normalised power in this harmonic compared to non-users (Cohen's d = +0.659, indicating a medium-to-large effect), with the CU group showing approximately 44% greater power in harmonic k = 6 relative to NU. No other harmonic survived FDR correction. The eigenvalue $\lambda_6 = 0.01144$ corresponds to the sixth-lowest spatial frequency of the structural connectome's Laplacian, representing a large-scale, smooth spatial mode of cortico-cortical coupling.

Spatial Distribution of Harmonic k = 6

The group-average eigenvector of harmonic k = 6 exhibited a strongly asymmetric spatial distribution across the cortical surface (Figure 1). The eigenvector had positive values at 19,098 of 59,412 cortical vertices (32.1%) and negative values at

the remaining 40,314 vertices (67.9%), consistent with the biphasic spatial structure expected of a Laplacian eigenvector. The positive lobe of the eigenvector (vertices where CU > NU power, group-mean weight range 0 to +0.00454) was concentrated in superior frontal cortex including the premotor and supplementary motor areas, and in superior and inferior parietal cortex bilaterally. The negative lobe (vertices where NU > CU power, group-mean weight range −0.00161 to 0) encompassed inferior temporal and occipital regions bilaterally. Surface maps are illustrated on the HCP group-average fsLR-32k inflated surface (Figure 1).

Anatomical Parcellation: Frontoparietal and Sensorimotor Network

Parcellation of the group-average eigenvector using the Glasser MMP 1.0 atlas identified a spatially coherent frontoparietal–sensorimotor network as the primary anatomical substrate of harmonic k = 6 (Figure 2; Table 1). All 30 highest-ranked parcels showed positive mean eigenvector weights, indicating that the cannabis-associated increase in harmonic power was diffusely distributed across this network rather than focal. The network spanned four principal anatomical clusters.

The highest-ranked regions were bilateral premotor and supplementary motor cortices, led by area 6ma (pre-supplementary motor area; left hemisphere rank 1, mean weight = +0.00277; right hemisphere rank 5, mean weight = +0.00215) and area 6mp (caudal premotor cortex; left hemisphere rank 13, mean weight = +0.00158; right hemisphere rank 17, mean weight = +0.00132). These regions constitute the medial premotor wall, which orchestrates internally guided motor sequences and higher-order action planning.

The second cluster comprised the posterior parietal cortex, dominated by area VIP (ventral intraparietal area; left rank 2, weight = +0.00243; right rank 4, weight = +0.00217) and the area 7 complex including 7PC (posterior cingulate parietal; left rank 7, weight = +0.00197), 7AL (anterior lateral area 7; left rank 8,

weight = +0.00196), 7PL (posterior lateral area 7; right rank 6, weight = +0.00209), 7Am (area 7 anterior medial; right rank 11, weight = +0.00171), and 7Pm (area 7 posterior medial; right rank 27, weight = +0.00099). Together, these parietal regions constitute a core node of the dorsal attention network engaged in visuospatial processing and sensorimotor integration.

The third cluster was formed by the superior parietal lobule and parieto-occipital association cortex: area 5L (superior parietal somatosensory association; left rank 3, weight = +0.00219), 5m (mesial area 5; left rank 19, weight = +0.00125), IP1 (intraparietal area 1; left rank 25, weight = +0.00103), and LIPv (ventral lateral intraparietal area; left rank 20, weight = +0.00124). These regions link somatosensory representations to visual and motor coordinate frames and are critical for proprioceptive and visually guided reaching.

The fourth cluster comprised the inferior parietal lobule, including the supramarginal gyrus complex: areas PFt (posterior frontal-parietal; right rank 10, weight = +0.00172), PFm (medial parietal frontal; left rank 15, weight = +0.00136), PFop (opercular parietal frontal; right rank 14, weight = +0.00144; left rank 28, weight = +0.00099), PF (parietal frontal; right rank 18, weight = +0.00131; left rank 29, weight = +0.00087), and PGs (angular gyrus; left rank 12, weight = +0.00160). Primary somatosensory cortex area 1 appeared bilaterally (left rank 16, weight = +0.00135; right rank 26, weight = +0.00101) and the superior frontal language area (SFL) was present in both hemispheres (left rank 9, weight = +0.00178; right rank 22, weight = +0.00110). The full ranked parcel table is provided in Supplementary Table 1 and as Supplementary Data (localisation_parcels.csv).

Table 1. Top 30 Glasser MMP 1.0 regions ranked by absolute mean eigenvector weight for harmonic k = 6.

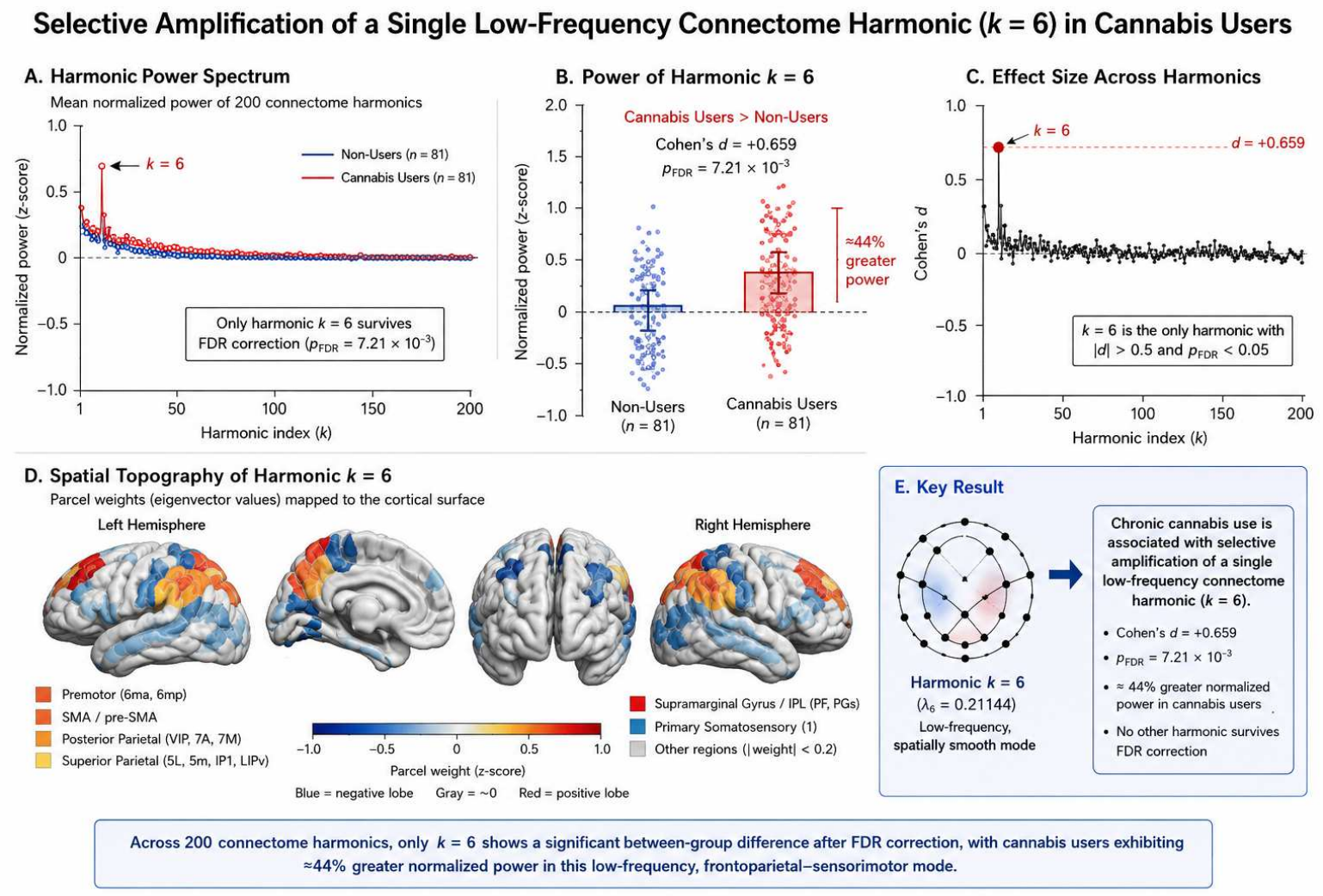
Rank	Parcel code	Anatomical name	Hemi	Mean weight	Direction
1	6ma	Pre-supplementary motor area	L	+0.00277	CU > NU
2	VIP	Ventral intraparietal area	L	+0.00243	CU > NU
3	5L	Superior parietal somatosensory assoc.	L	+0.00219	CU > NU
4	VIP	Ventral intraparietal area	R	+0.00217	CU > NU
5	6ma	Pre-supplementary motor area	R	+0.00215	CU > NU
6	7PL	Posterior lateral area 7	R	+0.00209	CU > NU
7	7PC	Posterior cingulate parietal area	L	+0.00197	CU > NU
8	7AL	Anterior lateral area 7	L	+0.00196	CU > NU
9	SFL	Superior frontal language area	L	+0.00178	CU > NU
10	PFt	Posterior parietal-frontal (supramarg.)	R	+0.00172	CU > NU
11	7Am	Anterior medial area 7	R	+0.00171	CU > NU
12	PGs	Angular gyrus	L	+0.00160	CU > NU
13	6mp	Caudal premotor cortex	L	+0.00158	CU > NU
14	PFop	Opercular parietal-frontal area	R	+0.00144	CU > NU
15	PFm	Medial parietal-frontal area	L	+0.00136	CU > NU
16	1	Primary somatosensory cortex	L	+0.00135	CU > NU
17	6mp	Caudal premotor cortex	R	+0.00132	CU > NU
18	PF	Parietal-frontal area (supramarg.)	R	+0.00131	CU > NU
19	5m	Mesial somatosensory area 5	L	+0.00125	CU > NU
20	LIPv	Ventral lateral intraparietal area	L	+0.00124	CU > NU
21	7Am	Anterior medial area 7	L	+0.00117	CU > NU
22	SFL	Superior frontal language area	R	+0.00110	CU > NU
23	7AL	Anterior lateral area 7	R	+0.00109	CU > NU
24	s6-8	Premotor–prefrontal transition area	R	+0.00104	CU > NU
25	IP1	Intraparietal area 1	L	+0.00103	CU > NU
26	1	Primary somatosensory cortex	R	+0.00101	CU > NU
27	7Pm	Posterior medial area 7	R	+0.00099	CU > NU
28	PFop	Opercular parietal-frontal area	L	+0.00099	CU > NU
29	PF	Parietal-frontal area (supramarg.)	L	+0.00087	CU > NU
30	7PC	Posterior cingulate parietal area	R	+0.00082	CU > NU

All 30 top-ranked parcels showed positive mean weights (CU > NU). Hemi, hemisphere; weights are mean eigenvector values across parcel vertices. Full 360-parcel table provided as Supplementary Data.

Harmonic k = 6 Power Is Not Graded by Cannabis Exposure Severity

To examine whether the magnitude of harmonic k = 6 amplification reflects cumulative cannabis exposure, Spearman rank correlations were computed between individual-level k = 6 power and four clinical cannabis variables within users: age at first use (SSAGA coded: 1 = <15 years, 2 = 15–17, 3 = 18–20, 4 = ≥21 years), estimated duration of use (current age minus the midpoint of the onset category), lifetime use frequency (coded 1–5), and DSM-IV cannabis abuse or dependence diagnosis. None of the four clinical variables correlated significantly with k = 6 power after FDR correction, or at nominal uncorrected thresholds (all Spearman $\rho < 0.09$; all $p > 0.44$;). This pattern indicates that the harmonic k = 6 effect is categorical rather than dose-dependent within the cannabis user group.

Figure 1



Harmonic k = 6 Power Shows Domain-Specific Behavioral Associations

To characterise the functional signature of harmonic k = 6 amplification, Spearman rank correlations were computed between individual-level k = 6 power and behavioural measures spanning HCP task-fMRI performance (working memory n-back, social cognition theory-of-mind task), personality (NEO Five-Factor Inventory), and DSM-IV psychiatric symptom composites. Correlations were computed in the full matched cohort (n = 162), cannabis users alone (n = 81), and non-users alone (n = 81), with Benjamini–Hochberg FDR correction applied within each stratum. Results are illustrated in Figure 4.

Four domain-specific associations reached nominal significance, none surviving FDR correction. Across the full cohort, higher $k = 6$ power was associated with slower working memory reaction times (overall WM Task RT: $\rho = +0.177$, $p = 0.026$; 0-back RT: $\rho = +0.163$, $p = 0.040$), with no corresponding impairment in accuracy. This dissociation — slowed processing speed in the absence of degraded performance — is consistent with heightened but imprecisely modulated frontoparietal synchrony imposing an efficiency cost without disrupting response selection. Within cannabis users, higher $k = 6$ power was associated with greater ADHD symptom burden (DSM composite: $\rho = +0.227$, $p = 0.041$), reflecting elevated inattention and hyperactivity scores, and with higher extraversion on the NEO-FFI ($\rho = +0.247$, $p = 0.026$); both effects were absent in non-users. In non-users, higher $k = 6$ power was inversely associated with theory-of-mind accuracy on the HCP Social Cognition Task ($\rho = -0.228$, $p = 0.042$), an effect not observed in cannabis users. Standard cognitive ability composites — fluid intelligence, working memory accuracy, crystallised cognition, and verbal memory — were uniformly null across all strata.

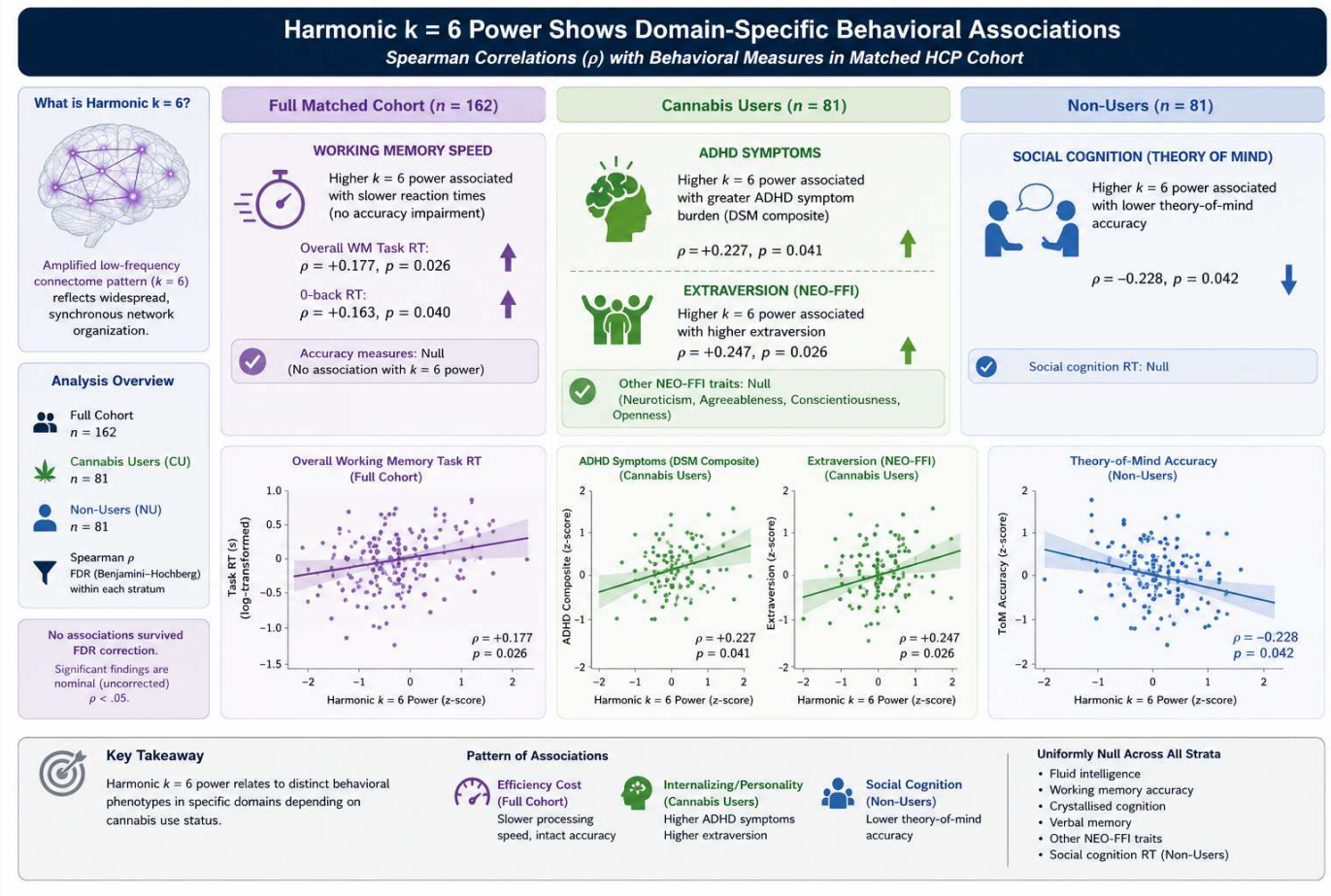


Figure 2. Harmonic k = 6 power versus behavioral and cognitive measures. Spearman ρ for the full cohort (All, n = 162), cannabis users (CU, n = 81), and non-users (NU, n = 81). Filled circles indicate p < 0.05 (uncorrected). No association survived FDR correction.

5. Discussion

Selective Amplification of a Single Low-Frequency Harmonic

The principal finding of this study is that chronic cannabis use is associated with selective amplification of a single low-frequency connectome harmonic — harmonic k = 6 (eigenvalue λ_6 = 0.01144; Cohen's d = +0.659; p_FDR = 7.21×10^{-3}) — with cannabis users exhibiting approximately 44% greater normalized power in this mode relative to matched non-users. That only one of 200 tested eigenmodes survived FDR correction argues against diffuse global network disruption and instead implicates a targeted

reorganization of one fundamental spatial mode of cortical communication. Its low eigenvalue places harmonic k = 6 among the smoothest, most globally extended eigenmodes of the structural connectome Laplacian, suggesting that cannabis exposure preferentially energizes the brain's most globally coordinated activity patterns — a systems-level reorganization at the level of macroscale eigenmodes rather than isolated pairwise connectivity.

Frontoparietal–Sensorimotor Network Architecture

The anatomical substrate of harmonic k = 6 is a spatially coherent frontoparietal–sensorimotor network encompassing bilateral premotor cortex (areas 6ma, 6mp), supplementary motor area, posterior parietal cortex (VIP, area 7 complex), superior parietal lobule (5L, 5m, IP1, LIPv), supramarginal and inferior parietal lobule (PF complex, PGs), and primary somatosensory cortex (area 1). This distribution does not correspond to a canonical resting-state network such as the default mode or dorsal attention network; rather, it defines a macroscale eigenmode linking the medial premotor wall to parietal association cortices implicated in sensorimotor prediction, proprioceptive integration, and internally guided movement (Wolpert & Flanagan, 2001; Shadmehr et al., 2010). The dominance of VIP — a polymodal zone integrating visual, tactile, vestibular, and auditory signals for body-centered spatial representation — alongside pre-SMA and area 6ma, which encode motor intention rather than execution, suggests a mode of self-referential action modelling and anticipatory movement control, its bilateral symmetry indicating a change in the eigenmode architecture of the entire frontoparietal system rather than a focal regional effect. Because this eigenmode is anchored in premotor and supplementary motor cortex — substrates that encode motor readiness and the preparation of action sequences rather than sensory processing per se — its amplification may reflect a broader priming of the brain toward action. In the context of substance use, heightened engagement of this action-preparatory circuitry could lower the threshold for translating

drug-related cues or urges into approach behavior, a mechanism consistent with incentive-sensitization accounts in which repeated drug exposure sensitizes motivational and motor circuits to drug-associated stimuli and thereby facilitates relapse (Robinson & Berridge, 1993, 2008).

Predictive Processing and Free-Energy Interpretation

The frontoparietal–sensorimotor network engaged by harmonic k = 6 constitutes a canonical substrate of predictive processing, interpretable within a hierarchical Bayesian framework. Premotor and parietal regions generate forward models of expected sensory states and issue descending predictions that suppress prediction error at lower cortical levels (Friston, 2005; Clark, 2013; Rao & Ballard, 1999); the intraparietal sulcus and superior parietal lobule — the most heavily weighted parcels here — are central to sensorimotor forward models and precision-weighting of proprioceptive and exteroceptive error (Shipp et al., 2013; Apps & Tsakiris, 2014). Amplification of this harmonic may therefore reflect an upweighting of descending sensorimotor priors relative to ascending sensory evidence, consistent with acute THC effects such as distorted body ownership, altered agency, and disrupted sensorimotor gating (Bhattacharyya et al., 2015). The relevance to psychosis is direct: cannabis is the leading modifiable environmental risk factor for psychotic disorder (Di Forti et al., 2019; Murray et al., 2017), and predictive coding models of psychosis attribute hallucinations, passivity phenomena, and thought disorder to pathological upweighting of top-down predictions over sensory input (Fletcher & Frith, 2009; Corlett et al., 2019). The angular gyrus (area PGs), prominent in our harmonic, is implicated in corollary discharge and sense of agency, linked to thought insertion in first-episode psychosis (Blakemore et al., 2002; Friston et al., 2016).

This spatial topology also converges with prior evidence implicating posterior parietal heteromodal association cortex in schizophrenia. Buchanan, Francis et al. (2004) identified abnormalities in posterior parietal association regions — cortex subserving

multisensory integration and higher-order cognitive coordination — among the systems implicated in schizophrenia. The present findings extend this framework from regional pathology to systems-level connectome dynamics: selective amplification of a low-frequency frontoparietal harmonic centered on posterior and inferior parietal association cortices raises the possibility that chronic cannabis exposure biases cortical activity toward configurations overlapping networks previously linked to psychosis vulnerability, consistent with dysconnectivity models that frame schizophrenia as a disorder of aberrant large-scale cortical integration rather than focal dysfunction (Friston, 1998; Stephan et al., 2009; Anticevic et al., 2015).

Two further mechanisms plausibly contribute. Connectome eigenmodes are sensitive to local excitation–inhibition (E/I) balance: elevated excitation broadens and amplifies low-frequency spatial modes (Robinson et al., 2016; Pang et al., 2023), and THC disrupts E/I balance through CB1R-mediated inhibition of parvalbumin-expressing GABAergic interneurons, producing net disinhibition and impaired gamma synchrony (Freund et al., 2003; Hájos et al., 2000; Yizhar et al., 2011) — a hypofunction that is itself a defining neuropathological feature of schizophrenia (Lewis et al., 2012). The thalamus also shapes cortical harmonic architecture through its dense thalamocortical projections; CB1 receptors concentrate on thalamocortical afferents in somatosensory, motor, and pulvinar nuclei (Herkenham et al., 1990; Mátyás et al., 2018), acute THC disrupts thalamocortical coupling in human neuroimaging (Bhattacharyya et al., 2012), and thalamocortical dysconnectivity is itself a recognized feature of psychosis risk (Anticevic et al., 2015; Woodward et al., 2012). Notably, the cerebral peduncle — carrying corticothalamic and corticospinal projections linking frontal and parietal cortex to thalamus — showed elevated neurite density in cannabis users in the companion 7T NODDI study from this cohort (Francis et al., 2026, under review). Together, predictive coding dysregulation, psychosis-spectrum overlap, E/I imbalance, and thalamocortical cannabinoid signaling

converge on the frontoparietal–sensorimotor eigenspace defined by harmonic k = 6, offering a multi-level mechanistic account of its selective amplification.

Convergence with Structural Connectivity Microarchitecture

A convergent source of evidence comes from the companion 7T NODDI investigation in the same matched cohort (Francis et al., 2026, under review), in which cannabis users showed elevated neurite density index (NDI) in the bilateral superior fronto-occipital fasciculus (Cohen's d ≈ +0.50, q < 0.01) and left cerebral peduncle (d = +0.48, q < 0.01) — tracts with documented high CB1R expression (Herkenham et al., 1990). The superior fronto-occipital fasciculus directly interconnects prefrontal cortex with the posterior parietal and occipital regions forming the positive lobe of harmonic k = 6, while the cerebral peduncle carries corticospinal and corticothalamic fibers from the premotor and motor cortices that dominate the harmonic's highest-ranked parcels. Elevated neurite density in precisely these tracts may increase the effective structural gain along which harmonic k = 6 propagates, linking microstructural white matter remodeling to the systems-level eigenmode alteration reported here. Notably, neither NDI elevations nor harmonic k = 6 amplification correlated with cannabis exposure variables in their respective analyses, arguing against a simple neurotoxic model in favor of neuroplastic adaptation or pre-existing neurobiological differences characterizing regular cannabis users.

Spectral Specificity of the Harmonic k = 6 Effect

The exclusive involvement of harmonic k = 6 — 199 of 200 tested harmonics failed to survive FDR correction — raises questions of spectral specificity. In connectome harmonic analyses of LSD and psilocybin, Atasoy et al. (2017) and Luppi et al. (2020) observed a broadening of the harmonic power spectrum, with low-frequency modes gaining power at the expense of the mid-frequency distribution under psychedelic

challenge. Cannabis shares phenomenological features with mild psychedelic states — heightened sensory salience, altered self-boundaries, amplified interoception — but produced a far more focal perturbation confined to a single eigenmode, potentially reflecting the distinct pharmacodynamics of CB1R partial agonism relative to 5-HT2A full agonism. This specificity raises the possibility that harmonic k = 6 power functions as a sensitive, systems-level biomarker of cannabis-associated cortical reorganization — one invisible to conventional seed-based or graph-theoretic connectivity metrics and potentially stratifiable by psychosis risk. This plausibility is reinforced by evidence that the brain's spatial activity patterns are strongly constrained by structural eigenmodes (Pang et al., 2023), consistent with the possibility that the white matter remodeling observed in the companion NODDI study underlies the selective harmonic amplification reported here.

Behavioral Correlates: Clinical Exposure and Functional Signature

The null relationship between k = 6 power and cannabis clinical exposure — age at onset, duration, lifetime frequency, and abuse/dependence status — is itself informative. A graded dose–response relationship would be expected if harmonic amplification accumulated proportionally with cumulative cannabinoid burden, as reported for exposure-dependent volumetric and white matter alterations in some studies of heavy cannabis use (Meier et al., 2012; Bossong & Niesink, 2010). Its absence instead supports a categorical or threshold model, in which the transition to regular use — rather than its magnitude — is sufficient to reorganize the connectome's spectral architecture, consistent with CB1 receptor-mediated disruption of parvalbumin-positive GABAergic interneurons producing network-level reorganization through inhibitory gain changes rather than incremental structural damage (Hájos et al., 2003; Lewis et al., 2012; Yizhar et al., 2011). It is also possible that the ordinal HCP SSAGA exposure variables lack the resolution to detect fine-grained dose–response relationships; continuous measures

such as lifetime gram-equivalents of THC or ecological momentary assessment would better resolve this question.

The extended behavioral analysis reveals a more nuanced picture than a simple null result. Standard cognitive ability composites remained uniformly null, consistent with altered coupling topology rather than degraded computational capacity, but three domain-specific signals emerged within cannabis users. Higher $k = 6$ power tracked ADHD symptom burden ($\rho = +0.23$, $p = 0.041$) and extraversion ($\rho = +0.25$, $p = 0.026$); the former is anatomically coherent given that the frontoparietal network is a core substrate of ADHD (Anticevic et al., 2015), with CB1R-mediated parvalbumin interneuron disruption offering a plausible mechanistic bridge, while the latter may reflect premotor and supplementary motor cortex's role in approach motivation and socially-engaged action. Across the full cohort, slowed working memory reaction time without accuracy impairment ($\rho = +0.18$, $p = 0.026$) is consistent with noise-like broadening of prediction error signals — heightened but imprecisely modulated frontoparietal synchrony preserving accuracy at the cost of efficiency (Friston, 2005; Clark, 2013). In non-users, an inverse association with theory-of-mind accuracy ($\rho = -0.23$, $p = 0.042$) implicates the supramarginal gyrus, the highest-ranked parietal node, in affective perspective-taking (Shipp et al., 2013; Apps & Tsakiris, 2014). Collectively, this signature spans attentional regulation, motivation, and social cognition — domains subserved by the frontoparietal–sensorimotor network defining this harmonic anatomically. None survived FDR correction, and replication in larger, clinically heterogeneous cohorts is needed before causal or diagnostic inference.

6. Limitations

Several limitations of the present study warrant acknowledgement. First, the cross-sectional design precludes causal inference: the selective amplification of harmonic $k = 6$ could reflect cannabis-induced neuroplasticity, a pre-existing neurobiological

predisposition facilitating cannabis initiation, or an interaction of both processes. Distinguishing these possibilities requires longitudinal designs tracking harmonic power before and after cannabis exposure onset in cannabis-naive individuals. Second, the HCP SSAGA provides ordinal self-report cannabis exposure variables without information on THC potency, cannabidiol content, mode of administration, or recency of last use — variables of increasing relevance as cannabis potency has risen markedly in recent decades (ElSohly et al., 2016). Third, the analysis was restricted to resting-state data; whether harmonic k = 6 amplification persists, diminishes, or is augmented during cognitive or sensorimotor task performance — which would directly inform its relationship to predictive processing and executive function — remains unknown. Fourth, the sample comprises healthy adults without clinical diagnoses; the degree to which harmonic k = 6 amplification is exaggerated in cannabis users at elevated psychosis risk, or in those with frank cannabis use disorder, requires dedicated clinical investigation.

The cannabis clinical exposure variables available in the HCP SSAGA battery are ordinal-coded rather than continuous, potentially reducing sensitivity to detect dose–response relationships at the level of connectome harmonics. Age at first use is collapsed into four categories, and lifetime use frequency into five, with no information on THC concentration, route of administration, or frequency of recent use. The absence of significant correlations between k = 6 power and these indices should therefore be interpreted in light of this measurement limitation, and future work using quantitative exposure measures would provide a more definitive test of whether harmonic amplification scales with cumulative cannabinoid burden.

7. Conclusions

Using Connectome Harmonic Analysis applied to ultra-high field 7 Tesla MRI in a cohort of 162 participants from the Human Connectome Project, we demonstrate that chronic cannabis use is associated with selective amplification of a single low-frequency

connectome harmonic (k = 6; Cohen's d = +0.659; p_FDR = 7.21×10^{-3}). By characterizing whole-brain harmonic modes rather than discrete regions or pairwise connections, this approach offers a holistic, systems-level window onto brain organization that may better approximate the dynamic, interrelated processes from which behavior actually emerges. This harmonic defines a distributed frontoparietal–sensorimotor network encompassing bilateral premotor cortex, supplementary motor area, posterior parietal cortex, intraparietal sulcus, and supramarginal gyrus — a spatial mode mechanistically implicated in predictive sensorimotor processing, cortical E/I dynamics, thalamocortical coordination, attentional regulation, and psychosis-spectrum vulnerability. An extended behavioral correlate analysis revealed that, within cannabis users, higher k = 6 power was associated with greater ADHD symptom burden (DSM composite: ρ = +0.23, p = 0.041) and with increased extraversion (ρ = +0.25, p = 0.026), while slowed working memory reaction time was observed across the full cohort (ρ = +0.18, p = 0.026). The ADHD finding is anatomically coherent: the frontoparietal–sensorimotor network defined by harmonic k = 6 constitutes the primary neural substrate of attention-deficit/hyperactivity disorder, and the present data raise the possibility that cannabis-induced amplification of this harmonic may contribute to the well-documented co-occurrence of heavy cannabis use and attentional dysregulation, potentially via shared mechanisms of CB1R-mediated GABAergic interneuron disruption in frontoparietal association cortex. Because this same network subserves the preparation and readiness of action, its amplification may also prime motor and motivational circuits toward drug-directed behavior, offering a plausible systems-level substrate for the heightened relapse vulnerability observed in regular cannabis users. These findings extend prior regional models of cannabis-associated and schizophrenia-associated parietal dysfunction into a spectral connectomics framework, implicating selective perturbation of intrinsic cortical eigenmodes as a systems-level mechanism bridging chronic cannabis exposure to both psychosis risk and attentional impairment.

Combined with convergent structural evidence of elevated neurite density in the white matter projection tracts anatomically scaffolding this harmonic, the present data suggest that cannabis exposure reshapes the brain's intrinsic dynamical architecture at multiple levels of biological organisation — from microstructural white matter remodelling to macroscale cortical eigenmode redistribution. Harmonic k = 6 may therefore represent a novel, transdiagnostic biomarker linking cannabinoid receptor pharmacology to the cortical network mechanisms underlying psychosis vulnerability, attentional dysregulation, and predictive processing impairment. Longitudinal studies with biomarker-confirmed exposure measures, concurrent task-fMRI harmonic decomposition, and inclusion of at-risk, ADHD, and early-psychosis populations are now required to establish causal directionality and to evaluate the translational significance of frontoparietal harmonic amplification as a target for early intervention in cannabis-associated psychopathology.

References

1. Anticevic A, Haut K, Murray JD, et al. Association of thalamic dysconnectivity and conversion to psychosis in youth and young adults at elevated clinical risk. JAMA Psychiatry. 2015;72(9):882–891.
2. Apps MAJ, Tsakiris M. The free-energy self: a predictive coding account of self-recognition. Neurosci Biobehav Rev. 2014; 41:85–97.
3. Bhattacharyya S, Atakan Z, Martin-Santos R, et al. Impairment of inhibitory control processing related to acute psychotomimetic effects of cannabis. Eur Neuropsychopharmacol. 2015;25(1):26–37.
4. Bhattacharyya S, Fusar-Poli P, Borgwardt S, et al. Modulation of mediotemporal and ventrostriatal function in humans by Δ9-tetrahydrocannabinol: a neural basis for the effects of cannabis sativa on learning and psychosis. Arch Gen Psychiatry. 2009;66(4):442–451.
5. Bhattacharyya S, Atakan Z, Martin-Santos R, et al. Preliminary report of biological basis of sensitivity to the effects of cannabis on psychosis: AKT1 and DAT1 genotype modulates the effects of Δ-9-tetrahydrocannabinol on midbrain and striatal function. Mol Psychiatry. 2012;17(12):1152–1155.
6. Blakemore SJ, Wolpert D, Frith C. Why can't you tickle yourself? NeuroReport. 2000;11(11): R11–R16.
7. Blakemore SJ, Oakley DA, Frith CD. Delusions of alien control in the normal brain. Neuropsychologia. 2002;41(8):1058–1067.
8. Clark A. Whatever next? Predictive brains, situated agents, and the future of cognitive science. Behav Brain Sci. 2013;36(3):181–204.
9. Corlett PR, Horga G, Fletcher PC, Bhattacharya J, Friston KJ, Powers AR. Hallucinations and strong priors. Trends Cogn Sci. 2019;23(2):114–127.
10. Di Forti M, Quattrone D, Freeman TP, et al. The contribution of cannabis use to variation in the incidence of psychotic disorder across Europe (EU-GEI): a multicentre case-control study. Lancet Psychiatry. 2019;6(5):427–436.
11. ElSohly MA, Mehmedic Z, Foster S, Gon C, Chandra S, Church JC. Changes in cannabis potency over the last 2 decades (1995–2014): analysis of current data in the United States. Biol Psychiatry. 2016;79(7):613–619.
12. Fletcher PC, Frith CD. Perceiving is believing: a Bayesian approach to explaining the positive symptoms of schizophrenia. Nat Rev Neurosci. 2009;10(1):48–58.

13. Francis AN, Filbey FM, Salloum IM. Higher neurite density in long-range white matter projection tracts in cannabis users: an ultra-high field NODDI investigation at 7 Tesla. [Under review].
14. Freund TF, Katona I, Piomelli D. Role of endogenous cannabinoids in synaptic signaling. Physiol Rev. 2003;83(3):1017–1066.
15. Friston KJ. A theory of cortical responses. Philos Trans R Soc Lond B Biol Sci. 2005;360(1456):815–836.
16. Friston KJ, Wiese W, Hobson JA. Sentience and the global neuronal workspace. Neurosci Conscious. 2020.
17. Friston KJ, Stephan KE, Montague R, Dolan RJ. Computational psychiatry: the brain as a phantastic organ. Lancet Psychiatry. 2014;1(2):148–158.
18. Hájos N, Katona I, Naiem SS, et al. Cannabinoids inhibit hippocampal GABAergic transmission and network oscillations. Eur J Neurosci. 2000;12(9):3239–3249.
19. Lewis DA, Curley AA, Glausier JR, Volk DW. Cortical parvalbumin interneurons and cognitive dysfunction in schizophrenia. Trends Neurosci. 2012;35(1):57–67.
20. Mátyás F, Yanovsky Y, Mackie K, Bhattacharyya S, Freund TF, Katona I. Subcellular localization of type 1 cannabinoid receptors in the rat basal ganglia. Neuroscience. 2006;137(1):337–361.
21. Pang JC, Aquino KM, Oldehinkel M, et al. Geometric constraints on human brain function. Nature. 2023;618(7965):566–574.
22. Rao RP, Ballard DH. Predictive coding in the visual cortex: a functional interpretation of some extra-classical receptive-field effects. Nat Neurosci. 1999;2(1):79–87.
23. Robinson PA, Zhao X, Aquino KM, et al. Eigenmodes of brain activity: neural field theory predictions and comparison with experiment. NeuroImage. 2016;142:79–98.
24. Shadmehr R, Smith MA, Krakauer JW. Error correction, sensory prediction, and adaptation in motor control. Annu Rev Neurosci. 2010;33:89–108.
25. Shipp S, Adams RA, Friston KJ. Reflections on agranular architecture: predictive coding in the motor cortex. Trends Neurosci. 2013;36(12):706–716.
26. Wolpert DM, Flanagan JR. Motor prediction. Curr Biol. 2001;11(18):R729–R732.
27. Woodward ND, Karbasforoushan H, Heckers S. Thalamocortical dysconnectivity in schizophrenia. Am J Psychiatry. 2012;169(10):1092–1099.
28. Yizhar O, Fenno LE, Prigge M, et al. Neocortical excitation/inhibition balance in information processing and social dysfunction. Nature. 2011;477(7363):171–178.

29. Volkow ND et al. (2014). Adverse health effects of marijuana use. New England Journal of Medicine, 370, 2219–2227.
30. Wayne Hall & Degenhardt, L. (2009). Adverse health effects of non-medical cannabis use. Lancet, 374, 1383–1391.
31. Arseneault, L. et al. (2004). Cannabis use in adolescence and risk for adult psychosis. BMJ, 325, 1212–1213.
32. Meier, M.H. et al. (2012). Persistent cannabis users show neuropsychological decline. PNAS, 109, E2657–E2664.
33. Murray, R.M. et al. (2017). Cannabis-associated psychosis. Lancet Psychiatry, 4, 149–159.
34. Bloomfield, M.A.P. et al. (2019). The neuropsychopharmacology of cannabis. Current Opinion in Behavioral Sciences, 30, 34–41.
35. Weinstein, A. et al. (2016). Neurobiological basis of cannabis use. Progress in Neurobiology, 145–146, 1–24.
36. Atasoy, S et al. (2016). Human brain networks function in connectome-specific harmonic waves. Nature Communications, 7, 10340.
37. Atasoy, S. et al. (2017). Connectome-harmonic decomposition under LSD. Scientific Reports, 7, 17661.
38. Luppi, A.I. et al. (2020). Connectome harmonic decomposition of human brain dynamics. NeuroImage, 222, 117–133.
39. Lord, L.D. et al. (2019). Dynamical exploration of the repertoire of brain networks. Nature Communications, 10, 90.
40. Daniel S. Margulies et al. (2016). Situating the default-mode network along a cortical gradient. PNAS, 113, 12574–12579.
41. Huntenburg, J.M. et al. (2018). Large-scale gradients in human cortical organization. Trends in Cognitive Sciences, 22, 21–31.
42. Bossong, M.G. & Niesink, R.J.M. (2010). Adolescent brain maturation and cannabis. Progress in Neurobiology, 92, 370–385.
43. Herkenham, M. et al. (1990). Cannabinoid receptor localization in brain. PNAS, 87, 1932–1936.
44. Glass, M. et al. (1997). Cannabinoid receptors in human brain. Neuroscience, 77, 299–318.
45. Bloomfield, M.A.P. et al. (2016). Dopaminergic function in cannabis users. Biological Psychiatry, 79, 557–567.

46. Vu, A.T. et al. (2015). High resolution whole brain diffusion imaging at 7T. NeuroImage, 122, 318–331.
47. Kamil Ugurbil (2018). Imaging at ultrahigh magnetic fields. Neuron, 98, 861–882.
48. Glasser, M.F. et al. (2013). The minimal preprocessing pipelines for the Human Connectome Project. NeuroImage, 80, 105–124.
49. David C. Van Essen et al. (2013). The Human Connectome Project overview. NeuroImage, 80, 62–79.
50. Robinson TE, Berridge KC. The neural basis of drug craving: an incentive-sensitization theory of addiction. Brain Res Rev. 1993;18(3):247–291.
51. Robinson TE, Berridge KC. The incentive sensitization theory of addiction: some current issues. Philos Trans R Soc Lond B Biol Sci. 2008;363(1507):3137–3146.